Eur Biophys J (2004) 33: 522–534
DOI 10.1007/s00249-004-0393-4

ARTICLE

Chartchalerm Isarankura Na Ayudhya
Virapong Prachayasittikul · Hans-Joachim Galla

Binding of chimeric metal-binding green fluorescent protein to lipid monolayer

Received: 11 November 2003 / Revised: 26 January 2004 / Accepted: 29 January 2004 / Published online: 2 March 2004

Abstract Membrane-based bioanalytical devices for metal determination using green fluorescent protein as the sensor molecule may be a useful future biomimetic material. However, in order to develop such a device, it is necessary first to understand the interaction of the protein with lipid membranes. Thus we have investigated the interaction between chimeric cadmium-binding green fluorescent proteins (CdBPGFPs) and lipid monolayers, using a film-balance technique complemented with epifluorescence microscopy. The binding avidity was monitored from the surface pressure vs. area isotherms or from the measured increase in the lateral pressure upon injection of the chimeric CdBPGFPs beneath the lipid monolayer. Increased fluidization as well as expansion of the surface area were shown to depend on the concentration of the CdBPGFPs. The kinetics of the protein-induced increase in lateral pressure was found to be biphasic. The chimeric CdBPGFPs possessed high affinity to the 1,2-dipalmitoyl-sn-glycero-3-phosphocholine (DPPC) monolayer with a dissociation constant of $K_d = 10^{-8}$M. Epifluorescence measurements showed that this affinity is due to the presence of the Cd-binding peptide, which caused the GFP to incorporate preferentially to the liquid phase and defect part of the rigid domain at low interfacial pressure. At high compression, the Cd-binding peptide could neither incorporate nor remain in the lipid core. However, specific orientation of the chimeric CdBPGFPs underneath the air–water interface was achieved, even under high surface pressure, when the proteins were applied to the metal-chelating lipid-containing surfaces. This specific binding could be controlled reversibly by the addition of metal ions or metal chelator. The reversible binding of the chimeric CdBPGFPs to metal-chelating lipids provided a potential approach for immobilization, orientation and lateral organization of a protein at the membrane interface. Furthermore, the feasibility of applying the chelator lipids for the codetermination of metal ions with specific ligands was also revealed. Our finding clearly demonstrates that a strong interaction, particularly with fluid lipid domains, could potentially be used for sensor development in the future.

Keywords Green fluorescent protein · Lipid monolayer · Film balance · Cadmium-binding peptide

Abbreviations GFP: green fluorescent protein · CdBPGFPs: cadmium-binding green fluorescent protein · DPPC: 1,2-dipalmitoyl-sn-glycero-3-phosphocholine · AAS: atomic absorption spectrometry · Cd^{2+}: cadmium (II) · Zn^{2+}: zinc (II) · Cu^{2+}: copper (II) · Ni^{2+}: nickel (II) · *E. coli*: *Escherichia coli* · NTA-DOGS: 1,2-dioleoyl-sn-glycero-3-(*N*-(5-amino-1-carboxypentyl iminodiacetic acid) succinyl) · His6GFP: hexahistidine green fluorescent protein · CdBP4GFP: four-repeat cadmium-binding peptide green fluorescent protein · His6CdBP4GFP: hexahistidine four-repeat cadmium-binding peptide green fluorescent protein · IMAC: immobilized-metal-affinity chromatography · PBS: phosphate-buffered saline · mN/m: millinewton per metre · le: liquid expanded · lc: liquid condensed · PE: phosphatidyl ethanolamine · PI: phosphatidyl inositol · NTA: nitrilotriacetic acid · EDTA: ethylenediamine tetraacetic acid · RESA: ring-infected erythrocyte surface antigen · CdBP: cadmium-binding peptide

C. Isarankura Na Ayudhya
V. Prachayasittikul (✉)
Department of Clinical Microbiology, Faculty of Medical Technology, Mahidol University, 2 Prannok Road, Bangkok-Noi, 10700 Bangkok, Thailand
E-mail: mtvpr@mucc.mahidol.ac.th
Tel.: +66-2-4197172
Fax: +66-2-4124110

C. Isarankura Na Ayudhya · H.-J. Galla (✉)
Institute of Biochemistry, Westfälische Wilhelms Universität, Wilhelm-Klemm-Str. 2, 48149 Muenster, Germany
E-mail: gallah@uni-muenster.de
Tel.: +49-251-8333200
Fax: +49-251-8333206

Introduction

Environmental contamination by toxic metals, particularly heavy metals, is of worldwide concern because of their extended persistence and numerous health risks to humans and animals. Electroplating plant, metal mining, nuclear wastes and electronic industries are major anthropogenic sources of metal pollution, releasing large amounts to the environment. At present, the standard method for metal determination is still focused on atomic absorption spectrometry (AAS) (Falchuk et al. 1988; Savory and Herman 1999). Although this method provides very high sensitivity for the detection of trace amounts of metal ions, it is costly and requires technical skill. Large-scale monitoring of toxic metal ions in biological systems and in the environment requires a rapid, inexpensive and simple quantification. Therefore, the development of analytical devices for metal determination represents a very significant breakthrough, capable of generating new concepts and technologies. These include the use of chemical compounds, selective electrodes, biological molecules or engineered cells and bioelectronics (Bontidean et al. 1998; Burdette et al. 2001; Choi et al. 2001; Javanbakht et al. 2000; Lehmann et al. 2000; Prachayasittikul et al. 2001; Prachayasittikul et al. 2000; Tauriainen et al. 1998).

A biosensor is an analytical device that converts a biological-sensing element into an electrical signal used to determine varieties of substances (for reviews, see Bakker and Telting-Diaz 2002; Cooper 2002; Keusgen 2002; Rishpon 2002; Vercoutere and Akeson 2002). Such a device is well established for providing high sensitivity and selectivity, particularly when the recognition elements such as receptors or antibodies are applied. Several methods for the incorporation or immobilization of such elements onto the sensor surfaces are available, e.g. covalent immobilization onto the polymer or onto polymerized lipids (Klee et al. 1995), as well as non-specific adsorption or immobilization onto lipid bilayers (Klee et al. 1992; Rogers et al. 1989). However, in some cases, little is known about how to immobilize the protein of interest onto the surface with high compatibility and allowing an application for sensor measurements.

From our previous findings, we have engineered a series of chimeric metal-binding green fluorescent proteins (chimeric GFPs), aiming to apply them for the development of protein and cell-based analytical devices for metal determination (Isarankura Na Ayudhya 2000; Prachayasittikul et al. 2001; Prachayasittikul et al. 2000). Owing to the autoilluminating activity of these proteins, direct quantification of metal ions by using purified chimeric GFPs became possible. However, we found that heavy metals exerted a suppressing effect on the fluorescence emission of the purified chimeric GFPs. Direct exposure of various concentrations of Cd^{2+} and related metals quantitatively reduced the intensity of the emitted fluorescence of the chimeric Cd-binding GFP. A linear reciprocal response has been shown at the nanomolar level of Cd^{2+}, with a correlation coefficient very close to one. Zn^{2+}, Cu^{2+} and Ni^{2+} exhibited a similar response, but in the micromolar range.

In contrast, quantification of metal ions via chimeric GFP-carrying *E. coli* revealed an enhancement of fluorescent intensity in the presence of Cd^{2+} and Zn^{2+}, but not with Cu^{2+}. A linear correspondence has been shown at the high nanomolar to high micromolar range of Cd^{2+} concentration. Such series of experimental data highlight the significant potential for future development of those protein and cell-based metal sensors that exhibit high sensitivity for metal determination. However, in order to obtain a better understanding of the interaction of chimeric proteins with cellular membranes, and for the future development of membrane-based metal sensors, it is necessary to understand the mechanism of the lipid–chimeric GFP interaction.

Here, we used the film-balance technique combined with fluorescence microscopy as an approach for studying the lipid–protein interaction at the air–water interface. The exploration of the interaction between the chimeric GFPs and lipid monolayers, as well as bilayers, subsequently revealed the feasibility of developing a membrane-based sensor device. The phospholipid monolayers were selected as the membrane model owing to their homogeneity and stability. In addition to their specific orientation in a planar geometry, the lipid monolayers provide a unique model membrane of great interest and reliability in understanding the incorporation property of a protein. Fluorescence microscopy allows the direct observation of the phase behaviour of the protein-containing lipid monolayer during compression if the autoilluminating chimeric GFPs are used. The lipid-binding avidity, as well as the molecular orientation of the chimeric GFPs onto the lipid monolayer, has been investigated; dissociation constants between the chimeric GFPs and lipid have been calculated in order to test the feasibility of applying these biofunctionalized membrane-based analytical devices for metal determination in the future. Metal-chelating lipids that are able to bind the chimeric GFPs, but only in the presence of the corresponding metal ions, have also been investigated since they may be used as receptor units.

Materials and methods

Lipids and chemicals

1,2-Dipalmitoyl-sn-glycero-3-phosphocholine (DPPC) and 1,2-dioleoyl-sn-glycero-3-(*N*-(5-amino-1-carboxypentyl iminodiacetic acid) succinyl) (NTA-DOGS) (Celia et al. 1999; Kubalek et al. 1998) were purchased from Avanti Polar Lipids Inc. (Alabaster, AL, USA) and were used without further purification. All solvents were of high-performance liquid chromatography grade from Merck (Darmstadt, Germany). Water was first purified through a millipore water purification system, Milli-Q RO 10 Plus (Millipore GmbH, Eschborn, Germany), and then finally with the millipore ultrapure water system, Milli-Q Plus 185 (18.2 $M\Omega\ cm^{-1}$). For all experiments, phosphate-buffered saline (50 mM Na_2HPO_4, 0.3 M

NaCl, pH 7.4; PBS) was used if not otherwise stated. Lipid stock solutions were prepared by dissolving powdered lipid in chloroform. As indicated in some experiments, the DPPC:NTA-DOGS (4:1) was preloaded with zinc ions (DPPC:NTA-DOGS-Zn^{2+}) by adding an equimolar amount of $ZnCl_2 \cdot 2H_2O$ dissolved in methanol.

Proteins

Chimeric metal-binding GFPs: His6GFP (Prachayasittikul et al. 2000); CdBP4GFP (Prachayasittikul et al. 2001) and His6CdBP4GFP (Prachayasittikul et. al., submitted) were expressed in *E. coli* strain TG1, and further purified to homogeneity by immobilized-metal-affinity chromatography (IMAC) charged with zinc ions as previously described.

Film-balance measurements

Surface pressure vs. area isotherms were obtained with a thermostatically controlled Langmuir film balance equipped with a Wilhelmy system. The filter paper was rinsed carefully with buffer to maintain its complete wettability. Monomolecular films were prepared, and the measurements were performed on a trough (Riegler and Kirstein, Mainz, Germany) with an operation area of 40 cm^2 and a bulk volume of 24 ml, kept at a temperature of 20 °C. The determination of the position and scanning speed of the film-balance barrier, as well as the recording of surface pressure vs. area isotherms, were computer-controlled. Prior to each experiment, the trough and barrier were cleaned with mucasol and dichloromethane followed by multiple repeated rinsing with deionized water. Phospholipid films of DPPC or DPPC:NTA-DOGS were prepared from a lipid stock solution by careful spreading via a microsyringe at the air–liquid interface.

After an equilibration time of 10 min, the film was compressed with a constant compression rate (5.81 cm^2/min) until the final surface pressure reached 10 mN/m. The interface was allowed to equilibrate for at least 30–45 min, at which point no further barrier movement was required to maintain constant pressure. All experiments were stirred continuously by a magnetic bar. Various concentrations of chimeric metal-binding GFPs dissolved in PBS were then injected into the subphase underneath the monolayer via an inlet port in the trough to yield subphase concentrations of 0–48 nM. Changes in lateral pressure after injection were measured at constant interfacial area and recorded for a minimum of 60 min. Data were fitted to the Michaelis-Menten equation (Knauer et al. 1997) using the non-linear regression program Sigma Plot (SPSS, Chicago, USA). The changes of pressure and the increasing velocity were applied by Lineweaver-Burke plot in order to investigate the dissociation constant between GFP and the lipid monolayer, in analogy to the previous works (Lu et al. 2002; Shank-Retzlaff et al. 1998). In addition, the isotherm characteristics before and after protein injection were determined. All measurements were performed at least two to three times to obtain reproducibility.

Epifluorescence measurements

The film-balance unit consisted essentially of an epifluorescence microscope, which was placed above a Langmuir trough. Fluorescence of the lipid monolayer (DPPC or DPPC:NTA-DOGS-Zn^{2+}) doped with the chimeric GFPs was excited and visualized via an epifluorescence microscope (Olympus STM5-MJS, Hamburg, Germany). The Langmuir trough carried a subphase volume of 76 ml PBS (pH 7.4). The trough, equipped with a computer-controlled movable barrier and a Wilhelmy system for the measurement of the surface tension, was placed on a specially designed stage (Riegler and Kirstein, Mainz, Germany) for the microscope. With the help of the remote-control stage, the trough could be moved independently in the three directions of the axes (*x, y, z*) of a Cartesian coordinate system, where the *x*- and *y*-axes were oriented perpendicular to the optical axis of the objective lens. For excitation, a high-pressure mercury lamp with a power of 50 W was used. Discrimination of excitation and emission light of the green fluorescent protein was achieved by corresponding cut-off filters. To form the monolayers, drops of the lipid stock solutions were formed at the tip of a Hamilton syringe and carefully spread to the air–liquid interface. The solvent was allowed to evaporate for at least 10 min.

After evaporation, the interface was compressed under a constant compression rate until the surface pressure reached about 5 mN/m. The chimeric GFP was then injected to the subphase without disturbance of the lipid monolayer, and the interface was further compressed up to 50 mN/m. The fluorescence pressure was recorded simultaneously by means of an SIT camera (Hamamatsu, Hamamatsu, Japan).

Results

Our previous findings indicated that the presence of Cd-binding peptide facilitated the incorporation of chimeric GFPs (CdBP4GFP and His6CdBP4GFP) into the inner lipid membrane of engineered *E. coli* cells (Prachayasittikul et al. 2001; Prachayasittikul et. al., submitted). Expelling the chimeric GFPs from the membrane required hazardous dissociation agents, e.g. 6 M guanidine hydrochloride prior to purification via IMAC. The purified chimeric GFPs were proven in preliminary investigations to have strong avidity to bind to lipid monolayers. Here, we focus on the mechanism of the interaction between the chimeric GFPs and lipid monolayers by using the film-balance technique as well as epifluorescence microscopy.

Effect of chimeric His6CdBP4GFP on the isotherms of the phospholipid monolayer

To study the degree of association of chimeric GFPs to lipid surfaces, DPPC model membranes, which provided both rigid and fluid domains, were selected. Fig. 1 demonstrates the effects of various concentrations of the chimeric His6CdBP4GFP on the isotherms

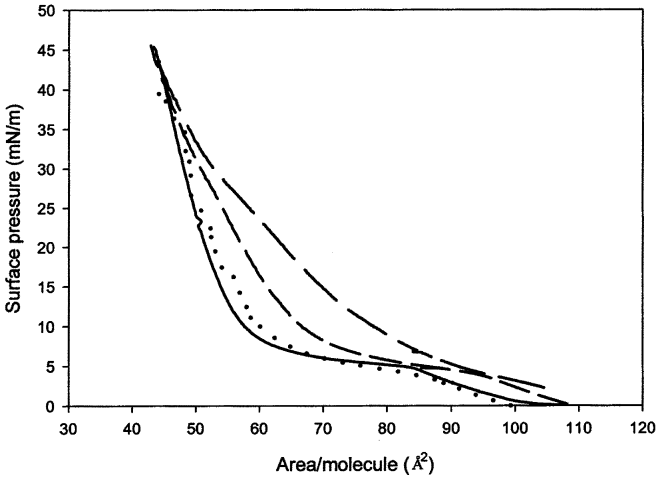

Fig. 1 Isotherms of the DPPC monolayer *(solid line)* in the presence of 3 nM *(dotted line)*, 18 nM *(short dashes)* and 48 nM *(long dashes)* of His6CdBP4GFP. The isotherms were measured at 20°C. Subphase was 50 mM Na_2HPO_4, 0.3 M NaCl, pH 7.4

of DPPC monolayers. The surface pressure vs. area isotherm of the pure DPPC showed the typical phase transition to be approximately 5 mN/m from the liquid-expanded (*le*) to the liquid-condensed (*lc*) phase. Injection of the chimeric His6CdBP4GFP (3, 18 and 48 nM) beneath the DPPC monolayer at 10 mN/m resulted in an increase in fluidity and in an expansion of the surface area of the lipid molecules. The increase in fluidity and the expansion of surface area were shown to be concentration-dependent. When the monolayer was highly compressed up to ~40 mN/m, the area per molecule became identical to that of a pure DPPC monolayer, even in the presence of the highest amount of protein applied. This supports the notion that at high surface pressure, the GFP is squeezed out from the lipid monolayer.

Epifluorescence measurements of binding between chimeric CdBPGFPs and the DPPC monolayer

To obtain a better understanding of the binding and molecular orientation of these chimeric GFPs in DPPC monolayers, the film-balance studies were complemented by epifluorescence microscopy. The monolayer was compressed to a pressure below the plateau region (5 mN/m) before injection of the protein. As shown in Fig. 2, epifluorescence of DPPC monolayers in the presence of His6CdBP4GFP after compression to 10, 20, 30, 40 and 50 mN/m was determined. Injection of the His6CdBP4GFP (18 nM) beneath the DPPC monolayer resulted in strong fluorescence emission at the fluid-phase domains (arrow B) and particularly in defect-rich parts at the rims of the rigid dark domains (arrow C in Fig. 2A). Upon further compression of the monolayer, the fluorescence intensity of the chimeric protein became more intense on the edges of DPPC solid domains owing to reduction of the fluid-phase area (Fig. 2B–D). However, when the pressure reached 50 mN/m, very low fluorescence intensity was observed (Fig. 2E). At such high pressure, the lipid density became so high that the peptide could neither incorporate nor remain in the lipid monolayer. These results inferred the preferential interaction of the Cd-binding peptide to the phospholipid in the liquid-phase and to defects at the border in the solid-phase domains.

To confirm whether the Cd-binding region played a role in the incorporation of the chimeric GFP to the DPPC monolayer, the chimeric His6GFP was investigated for comparison. Figure 3A exhibits an epifluorescence measurement of a DPPC monolayer compressed to 10 mN/m in the presence of 18 nM His6GFP. This photograph clearly shows that only very low fluorescence intensity is present in the fluid areas. Such low intensity was still detected up to a compression of 15 mN/m. Increasing the His6GFP concentration up to 85 nM achieved the same result (Fig. 3B). Addition of 18 nM His6CdBP4GFP to the subphase of the monolayer preincubated with 85 nM His6GFP at 15 mN/m did not result in the fluorescence pattern typical for His6CdBP4GFP. This clearly shows that the surface is fully occupied with non-specifically adsorbed His6GFP due to its large excess.

Competitive binding between chimeric His6CdBP4GFP and His6GFP to the DPPC monolayer

To further investigate the binding of His6GFP and His6CdBP4GFP to the DPPC monolayer, experiments were initiated by injecting His6CdBP4GFP underneath the monolayer followed by an addition of His6GFP. As

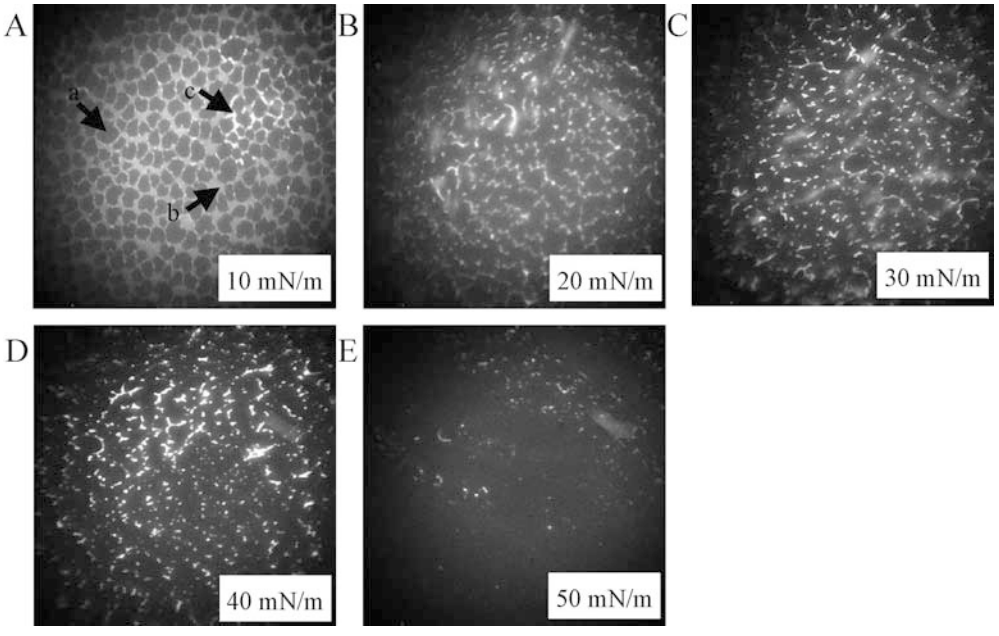

Fig. 2 Epifluorescence measurements of the DPPC monolayer in the presence of 18 nM of His6CdBP4GFP compressed at different surface pressures (10–50 mN/m; **A–E**). *Arrow A* indicates solid domain. *Arrows B* and *C* indicate binding avidity of the chimeric His6CdBP4GFP to the liquid phase and the defect part of the solid domain, respectively. Subphase was 50 mM Na_2HPO_4, 0.3 M NaCl, pH 7.4

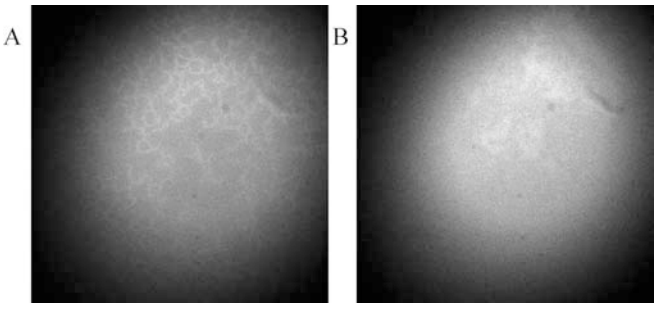

Fig. 3 Epifluorescence measurements of the DPPC monolayer in the presence of 18 nM (**A**) and 85 nM (**B**) of His6GFP. The monolayer was compressed at 10 mN/m. Subphase was 50 mM Na_2HPO_4, 0.3 M NaCl, pH 7.4

shown in Fig. 4A, the strong fluorescence emission at the fluid areas was detected if only His6CdBP4GFP was present. Upon adding 18 nM His6GFP, a decrease in fluorescence intensity was observed (Fig. 4B). Injection of additional His6GFP up to 180 nM resulted in a greater suppression of the fluorescence (Fig. 4C). The monolayer was then further compressed in order to test whether the His6CdBP4GFP could regain its fluorescence intensity (Fig. 4D). Interestingly, recovery of strong fluorescence intensity could be observed readily at high compression (30 mN/m; Fig. 4E). However, further compression of the monolayer caused the fluorescence intensity to decrease (Fig. 4F, G). This indicates the multiple avidity that could be competed by His6GFP, while the higher-binding avidity regained the binding to the lipid monolayer at higher compression.

Fig. 4A–G Epifluorescence measurements of competitive binding between chimeric His6CdBP4GFP and His6GFP to the DPPC monolayer. The monolayer was compressed at 5 mN/m, then 18 nM of chimeric His6CdBP4GFP was injected into the subphase. The monolayer was continued to be compressed at 10 mN/m and kept constant (**A**). His6GFP was subsequently injected beneath the monolayer to yield the subphase concentration of 18 nM (**B**) and 180 nM (**C**). The monolayer was then compressed at 20–50 mN/m (**D–G**). Subphase was 50 mM Na_2HPO_4, 0.3 M NaCl, pH 7.4

Enhancement of interfacial pressure of the DPPC monolayer by Cd-binding GFPs

DPPC monolayers were prepared, and lateral pressure was kept constant at 10 mN/m followed by injection of CdBP4GFP and His6CdBP4GFP. For comparison, His6GFP was applied as control. The increase in interfacial pressure with time at the desired lateral pressure was taken to monitor the degree of incorporation. The presence of Cd-binding peptide caused two steps (biphasic kinetics) of increasing lateral pressure. A dramatic pressure increase of 3–4 mN/m was observed within 5 min, followed by a gradual increase until saturation was reached within 15–20 min in the case of the CdBP4GFP (Fig. 5B). A similar biphasic increase in pressure was also observed when His6CdBP4GFP was injected (Fig. 5C).

Changes in rate and magnitude of the surface pressure during the first step as well as the second step were found to be dependent on the subphase protein concentration. The His6CdBP4GFP provided a more potent effect than the CdBP4GFP. The highest change of pressure was found to be approximately 1 mN/m higher compared with CdBP4GFP, particularly at concentrations greater than 18 nM. In contrast, the addition of various concentrations of His6GFP (3–48 nM) caused only a one-step increase in the lateral pressure and with a lower magnitude. A gradual increase in pressure could potentially be achieved according to time and concentration of the protein. The highest change of pressure reached almost saturation within 30–35 min and was followed only by a further slow increase in pressure, possibly due to multilayer adsorption of protein to the lipid membrane as shown in Fig. 5A.

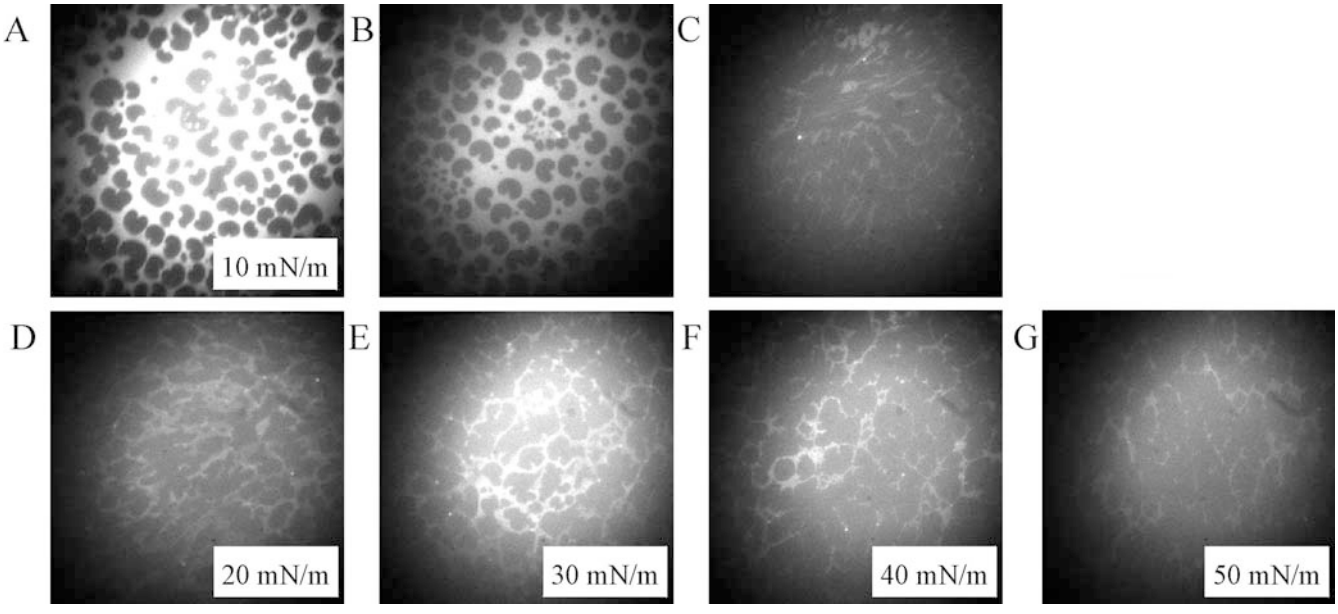

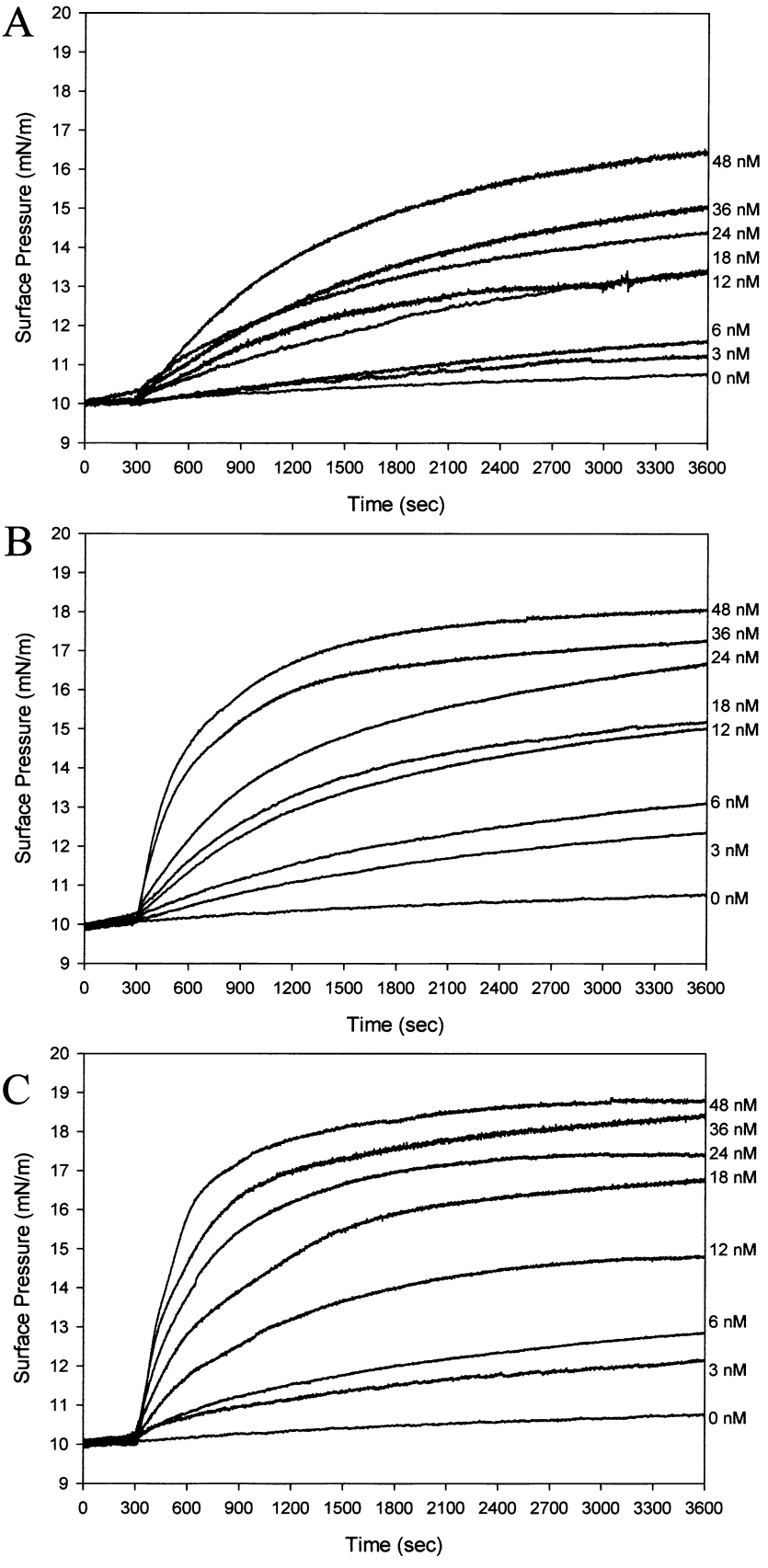

Fig. 5 Effect of various concentrations (3–48 nM) of chimeric His6GFP (**A**), CdBP4GFP (**B**) and His6CdBP4GFP (**C**) on the interfacial pressure of the DPPC monolayer. The monolayer was compressed until the pressure reached 10 mN/m, and the interface was allowed to equilibrate for at least 30–45 min; the movable barrier then was stopped. After 5 min, chimeric GFP was injected into the subphase. Changes of pressure were recorded for 60 min. The value given was the average of two independent samples. Subphase was 50 mM Na_2HPO_4, 0.3 M NaCl, pH 7.4

Analysis of dissociation constants of the Cd-binding GFPs to the DPPC monolayer

To provide further evidence for a specific interaction, dissociation constants of the Cd-binding GFPs to the DPPC monolayer were determined. This analysis was derived from plots of the delta pressure (deltaP) or velocity against protein concentration (Figs. 6 and 7). In Fig. 6A, the maximum change of lateral pressure is plotted versus concentrations of the chimeric GFPs. The deltaP values caused by both the CdBP4GFP and His6CdBP4GFP exceed that of the His6GFP at all concentrations tested. At the highest concentration (48 nM), the deltaP values were 7, 8 and 5.5 mN/m for the CdBP4GFP, His6CdBP4GFP and His6GFP, respectively. These binding curves given in Fig. 6A were subsequently fitted to yield the dissociation constants according to the Lineweaver-Burke equation (Lu et al. 2002). As shown in Fig. 6B, the dissociation constants of the CdBP4GFP, His6CdBP4GFP and His6GFP to DPPC monolayers were 1.6×10^{-8} M, 2.5×10^{-8} M and 1.0×10^{-6} M, respectively.

Owing to the biphasic responses upon addition of the chimeric Cd-binding GFPs to the monolayer, the initial velocities of the first and second steps were plotted versus the protein concentration (Fig. 7A, C). The initial velocity at the first step increased in the order His6CdBP4GFP > CdBP4GFP > His6GFP, while, in contrast, the corresponding dissociation constants to DPPC were in the same range ($\sim10^{-7}$ M) (Fig. 7B). CdBP4GFP and His6CdBP4GFP caused the second step of monolayer expansion for which the dissociation constants to DPPC of these two chimeric proteins were further calculated. As represented in Fig. 7D, the dissociation constants for CdBP4GFP and His6CdBP4GFP to DPPC monolayers were 1.1×10^{-8} and 2.6×10^{-8} M, respectively. Values were close to the values determined by the corresponding plot of the deltaP values (Fig. 6B).

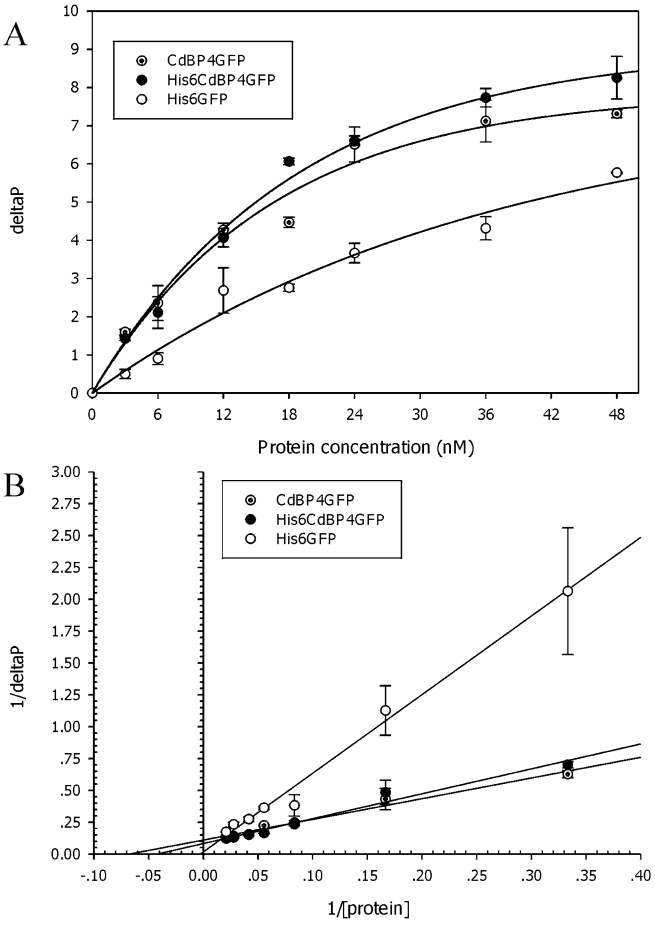

Fig. 6 Analysis of dissociation constant between the chimeric GFPs and the DPPC monolayer as calculated from delta pressure (deltaP) versus protein concentration (nM) (**A**). The results were further fitted to the Lineweaver-Burke plot (**B**). The value given was the average of two independent samples

Effect of cadmium ions on fluorescence emission of incorporated chimeric His6CdBP4GFP onto the DPPC monolayer

To evaluate whether the incorporation of the chimeric His6CdBP4GFP into the DPPC monolayer could be suited for further applications as a membrane-based analytical device for metal determination, the effect of metal ions, particularly cadmium ions, on the fluorescence emission of incorporated chimeric His6CdBP4GFP was determined. Again, the DPPC monolayer was selected to be a supporter membrane owing to its low adsorption of cadmium ions compared with the other phospholipids, e.g. PS and PI (Bevan et al. 1983; Deleers et al. 1986; Girault et al. 1998; Lis et al. 1981; Tacnet et al. 1991). No significant difference in fluorescence emission between time 0 and time 60 min was found. When the monolayer was continuously compressed up to 50 mN/m, a typical pattern of His6CdBP4GFP to the DPPC monolayer was observed (as, for example, in Fig. 2). It should be noted that some of the cadmium ions formed complexes with the remaining protein in the subphase, as evidenced by the precipitation of chimeric protein beneath the lipid monolayer.

Specific orientation of the His6CdBP4GFP onto the metal-chelating lipid monolayer

To investigate whether the presence of Cd-binding peptide facilitated a specific orientation of the chimeric GFPs onto the lipid monolayer, the metal-chelating lipid (NTA-DOGS) was used as a receptor unit. The NTA-DOGS was mixed together with the DPPC in an appropriate ratio (DPPC:NTA-DOGS; 4:1). Figure 8 demonstrates the isotherms of the lipid mixture compared with the pure DPPC. The isotherm of the lipid mixture exhibited a characteristic where the phase transition is still visible but the membrane gained more fluidity. The isotherm was shifted to a higher surface

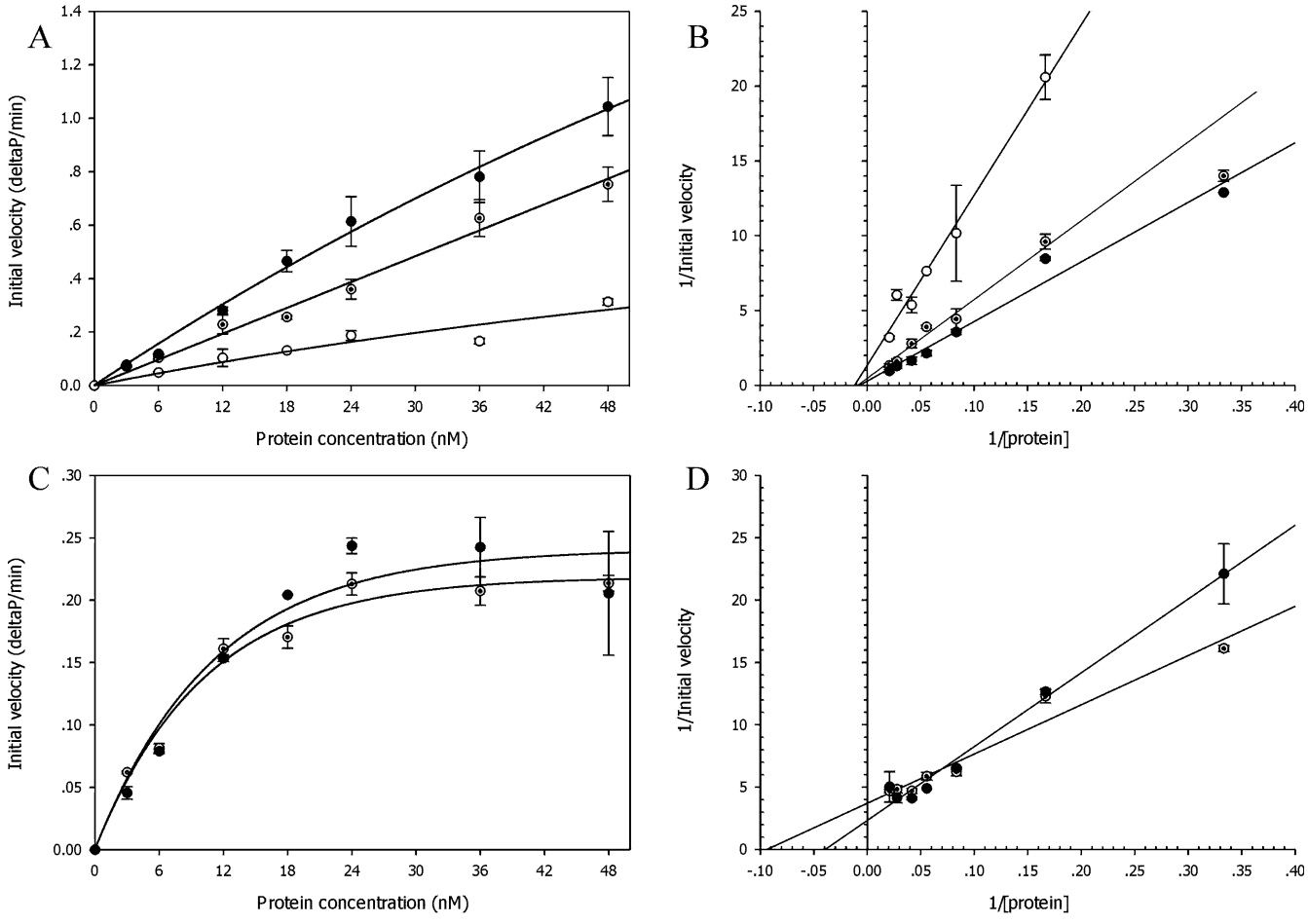

Fig. 7 Analysis of dissociation constant between the chimeric GFPs and the DPPC monolayer as calculated from initial velocity (deltaP/min) of first step (**A**) or second step (**C**) in biphasic curve versus protein concentration (nM). All results from the first and second steps were fitted to the Lineweaver-Burke plot as represented in **B** and **D**, respectively. The value given was the average of two independent samples

pressure and, additionally, the plateau region became less horizontal compared with pure DPPC monolayers, owing to fluidization as a result of the NTA-DOGS. Addition of metal ions (Zn^{2+}) to monolayers of pure metal-chelating lipid did not cause any significant difference in the isotherm (data not shown). In the mixed lipid monolayer, the endpoint of the *lc–le*-transition was shifted to higher pressure, clearly evidencing a phase separation.

The His6CdBP4GFP (18 nM) was then injected beneath the lipid monolayer. The isotherm became more smooth, and the phase transition less pronounced. As shown in Fig. 9A, strong fluorescence intensity could be observed in the liquid phase, even under high pressure up to 50 mN/m. Similar observations were made with the CdBP4GFP (data not shown) and, even more importantly, the addition of the His6GFP into the subphase exhibited the same phenomenon as represented in Fig. 9B.

To further confirm that the orientation of the His6CdBP4GFP or His6GFP at the membrane interface is caused by specific interaction between the metal-binding sites and the immobilized metal ions at the NTA head group, the same experiment was performed in PBS buffer supplemented with 5 mM EDTA. Again, strong fluorescence could be detected upon addition of the His6CdBP4GFP due to the presence of the Cd-binding peptide, which caused the protein to be incorporated into the fluid lipid domains.

When the monolayer was further compressed, a marked decrease in fluorescence was detected (Fig. 10C–E). Similar observations were also made in the case of the CdBP4GFP (data not shown). In contrast, very low fluorescence intensity at low surface pressure could be detected in the case of His6GFP (Fig. 10F). All these findings indicate that specific orientation of the chimeric GFPs onto the lipid monolayer was mediated by the metal-binding lipid. Membrane regions enriched with this lipid would provide binding avidity of the chimeric GFPs to the lipid monolayer via its hydrophobicity, without participation of the metal. However, if metal is available, the membrane avidity is dominated by protein binding to the chelated metal. Thus, protein binding to the chelating site is stronger than the hydrophobic interaction of the Cd-binding GFPs with fluid lipid domains.

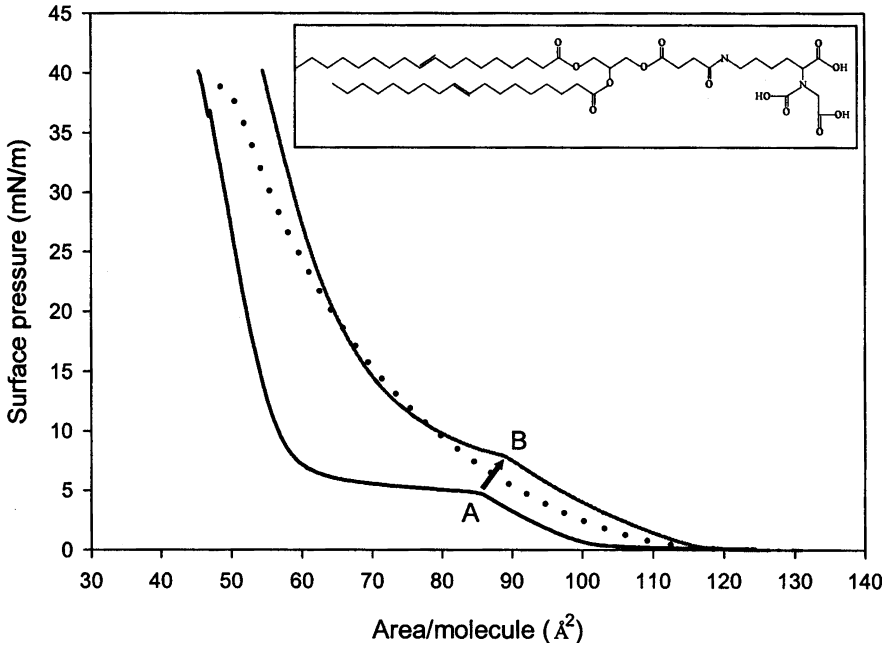

Fig. 8 Isotherms of the DPPC monolayer *(solid line A)*, NTA-DOGS monolayer *(dotted line)* and DPPC:NTA-DOGS (4:1) monolayer *(solid line B)* determined at 20 °C. Subphase was 50 mM Na_2HPO_4, 0.3 M NaCl, pH 7.4. *Inset* indicates a structure of NTA-DOGS

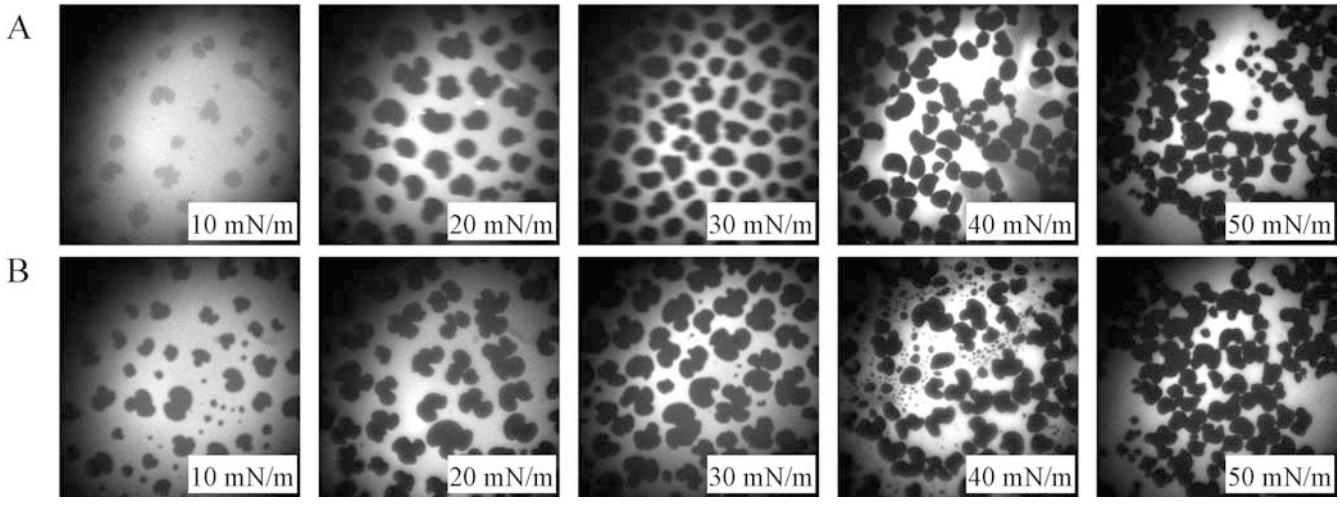

Fig. 9 Epifluorescence measurements of lipid mixture (DPPC:NTA-DOGS; 4:1) charged with equimolar amount of $ZnCl_2$ in the presence of 18 nM His6CdBP4GFP (**A**) or His6GFP (**B**) compressed at 10–50 mN/m. Subphase was 50 mM Na_2HPO_4, 0.3 M NaCl, pH 7.4

Similarity of the Cd-binding peptide to other proteins

To compare the Cd-binding sequence to other peptides in nature, alignment of protein sequences was performed using the CLUSTALW (Thompson et al. 1994) linked to the Bioedit program. As presented in Fig. 11, both the Cd-binding peptide (CdBP4) and the hexapolyhistidine fused to the Cd-binding peptide (His6CdBP4) exhibited sequences similar to those shown by two kinds of natural protein; PFB0920w (protein with DnaJ domain (RESA like) from *Plasmodium falciparum*) (Gardner et al. 1998) and Magainin 1 and 2 (antimicrobial peptide from *Xenopus laevis*) (Matsuzaki et al. 1997). The former protein was referred to be a hypothetical protein with unknown function. This protein consists of the DnaJ domain and a large non-globular domain. A predictable function of this protein is probably similar to that of the DnaJ-domain superfamily and RESA-like (ring-infected erythrocyte surface antigen). The DnaJ domains act as cofactors for HSP70-type molecular chaperons and participate in protein folding and trafficking, intracellular transport of proteins, complex assembly, organelle biosynthesis and initiation of translation (Cyr et al. 1994).

RESA is known to provide binding avidity to the cytoplasmic side of the erythrocyte membrane, with the membrane skeleton component spectrin as a major site of binding. Furthermore, the RESA might be involved in

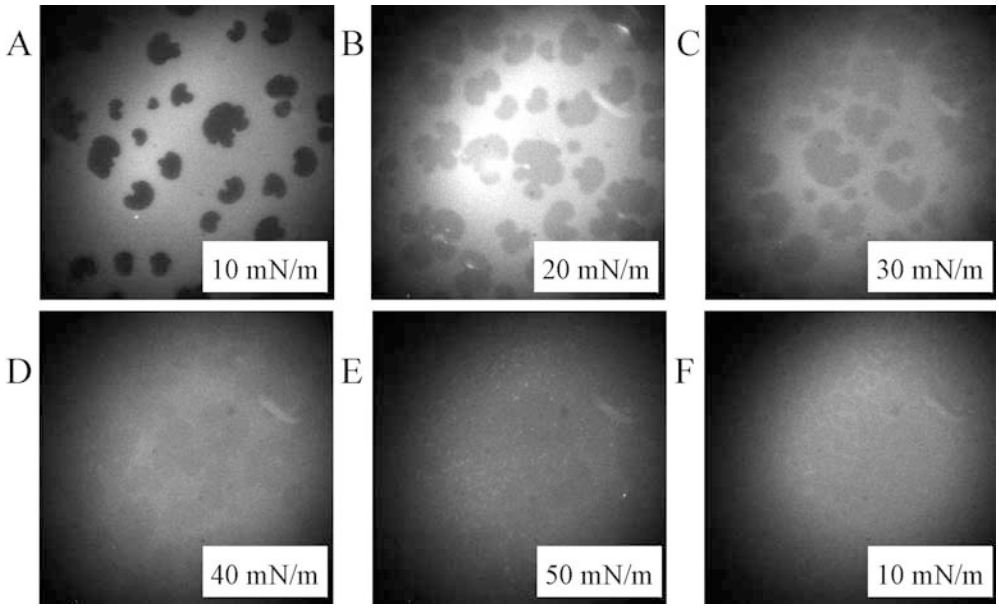

Fig. 10 Epifluorescence measurements of lipid mixture (DPPC:NTA-DOGS; 4:1) charged with equimolar amount of $ZnCl_2$ in the presence of 18 nM His6CdBP4GFP compressed at different pressures (**A–E**) or His6GFP compressed at 10 mN/m (**F**). Subphase was 50 mM Na_2HPO_4, 0.3 M NaCl, 5 mM EDTA, pH 7.4

A

```
CdBP4            ------TMITPSL------MSSHSQKVFHSQKVFHSQKVFHSQKV-----FAVP-----------VEK------  Identity = 20/40 (50%); Similarity = 22/40 (55%)
His6CdBP4        ------TMITPSLHHHHHHASSHSQKVFHSQKVFHSQKVFHSQKV-----FAVP-----------VEK------  Identity = 20/46 (43%); Similarity = 22/46 (48%)
PFB0920w         EKLNHSEKLNHSEKVNHSEKVNHSEKVNHSEKVNHSEKVNHSEKLNHPNREKHSQKEKHTEKDDKRNN
Consensus/100%          h  S          HS KV HS KV HS KV HS KV     h  P             EK
```

B

```
CdBP4            TMITPSL------MSSHSQKVFHSQKVFHSQKVFHSQKVFAVPVEK
His6CdBP4        TMITPSLHHHHHHASSHSQKVFHSQKVFHSQKVFHSQKVFAVPVEK  Identity = 6/23 (26%); Similarity = 14/23 (61%)
Magainin 1       -----GI-----------GKFLHSAGKFG--KAFVG-EIMKS----
Magainin 2       -----GI-----------GKFLHSAKKFG--KAFVG-EIMQS----
Consensus/100%         h            KhhHS   F   KhF u chh
```

Fig. 11 Sequence alignments between the Cd-binding peptide (CdBP4) or hexapolyhistidine fused to the Cd-binding peptide (His6CdBP4) and the PFB0920w-encoding protein with DnaJ domain (RESA-like; ring-infected erythrocyte surface antigen from *P. falciparum*; genbank accession no. gi7494396) (**A**) or Magainin 1 and 2 (antimicrobial peptide from African frog skin; *Xenopus laevis*) (**B**). The alignment was constructed by the profile alignment option of CLUSTALW linked to the Bioedit program. *h* indicates hydrophobic residues (A, C, F, I, L, M, V, W and Y); *u* indicates "minute" residues (G, A and S); *c* indicates charged residues (D, E, K and R). Gaps were introduced to optimize alignment

stabilization of the erythrocyte membrane during thermal denaturation via heat-induced fragmentation (Da Silva et al. 1994). The magainin peptides possess antimicrobial activity with low toxicity to normal eukaryotic cells. The mechanism of action is considered to enhance the permeability of bacterial membranes. Percentages of identity and similarity of the CdBP4 compared with the amino acid residues 500–560 of the PFB0920w were calculated to be 50% and 55%, while the His6CdBP4 showed 43% and 48%, respectively (Fig. 11A). In addition, both sequences of the Cd-binding peptide also possessed 26% and 61% identity and similarity compared with the magainin 1 and 2 (Fig. 11B).

Discussion

We explored the detailed binding properties of the cadmium-binding green fluorescent proteins and lipid monolayers using the film-balance technique and epifluorescence microscopy. These include effects of the chimeric proteins on the isotherms of lipid monolayers, changes of interfacial pressure upon addition of the chimeric proteins and analysis of dissociation constants between the chimeric proteins and the lipid monolayer. Furthermore, the peptide–lipid binding, as well as the molecular organization of the chimeric proteins onto the lipid monolayer, were investigated. These findings indicate that there is a potential for the future development of a membrane-based bioanalytical device for metal determination.

Lipid-binding avidity of the chimeric cadmium-binding green fluorescent protein

In this study, we first investigated the role of Cd-binding peptide (CdBP) on the binding avidity of the green fluo-

rescent protein (GFP) to lipid monolayers. The Cd-binding peptide was previously derived from phage-display technology (Mejare et al. 1998). This peptide was successfully fused to the GFP and applied as a potential tool for metal determination (Prachayasittikul et al. 2001). In a previous study, we found that engineered *E. coli* cells expressing chimeric four-Cd-binding regions fused to GFP (CdBP4GFP), and the GFP having hexapolyhistidine in combination with four-regions Cd-binding peptide (His6CdBP4GFP), exhibited different characteristics of fluorescence emission (Prachayasittikul et al., submitted). The chimeric CdBP4GFP and His6CdBP4GFP were found to localize in the membrane debris, while the hexahistidine GFP (His6GFP) and the native GFP were expressed as cytoplasmic proteins. Owing to the strong interaction between the chimeric protein and the membrane, expulsion of the CdBP4GFP and the His6CdBP4GFP required a strong dissociation agent, e.g. 6 M guanidine hydrochloride.

The strong affinity to lipid has been significantly evidenced in this study. The CdBP4GFP and the His6CdBP4GFP displayed remarkable high affinity for DPPC monolayers, approximately two orders of magnitude higher than that of the His6GFP, as has been calculated from the measured pressure increase upon protein addition (Fig. 6). Moreover, incorporation of the CdBPGFPs to lipid monolayers demonstrated biphasic kinetics as in the case of Cytochrome P450 2B4, Melittin, Polymyxin B and other substances (Dufourcq and Faucon 1977; Kahle et al. 1996; Maman et al. 1999; Shank-Retzlaff et al. 1998).

A rapid initial increase in surface pressure followed by a more gradual increase over time was observed. Apparent binding constants, calculated from the intercept of double reciprocal plots between the velocity of pressure increasing at the first phase and the protein concentration, were at the 10^{-7} M-level for all three chimeric proteins (His6GFP, CdBP4GFP and His6CdBP4GFP). However, the dissociation constant at the second step was 10^{-8} M for the CdBP4GFP and His6CdBP4GFP (Fig. 7). All these findings clearly indicated that the first-step interaction is caused by non-specific adsorption of the integral part of GFP to all areas in the lipid monolayer, while the second step might be caused by the incorporation of the Cd-binding peptide into the fluid phase of the lipid monolayers. This evidence is in good agreement with the binding interaction of CdBPGFPs with lipid monolayers observed by epifluorescence microscopy (Figs. 2 and 3).

Molecular orientation of the chimeric cadmium-binding green fluorescent protein at the membrane interface

Fluorescence spectroscopy is a highly sensitive technique which is used extensively to study peptide–lipid binding and peptide incorporation into membranes (Dietrich et al. 1995; Grandbois et al. 1996). This technique was applied in order to study the molecular orientation of the chimeric Cd-binding GFPs at the membrane interfaces of either DPPC monolayers or metal-chelating lipid-containing membranes (DPPC:NTA-DOGS-Zn^{2+}; 4:1). On the DPPC monolayer, both the CdBP4GFP and the His6CdBP4GFP exhibited stronger fluorescence intensity at the liquid phase and the defect part of the rigid domain than the His6GFP. The fluorescence of the adsorbed His6GFP vanished in a few seconds without a decrease in lateral pressure. This indicates that the His6GFP denatures after adsorption owing to very high pressure at the air–water interface (Dorn et al. 1998; MacRitchie 1986; Norde 1986; Schmidt et al. 1990).

This observation suggests that the CdBP4GFP or the His6CdBP4GFP have a conformation that allows the GFP to remain in the outer aqueous phase, while the Cd-binding peptide is incorporated into the lipid core. However, at high compression, the Cd-binding peptide could neither incorporate nor remain in the lipid core. In contrast, specific orientation of the chimeric GFPs was achieved upon applying the proteins onto the metal-chelating lipid. This orientation was proven to be due to specific metal-binding avidity of either the Cd-binding peptide or the hexapolyhistidine to immobilized zinc ions on the NTA head groups of lipid. Specific binding of the chimeric GFPs to metal ions resulted in correct protein folding and caused the protein to localize underneath the air–water interface. Therefore, strong fluorescence intensity could be detected in the liquid phase even under high compression (Fig. 9). The fluorescence emission can be abolished upon addition of metal-chelating agent (EDTA) into the subphase. However, it is noteworthy that the presence of Cd-binding peptide can reincorporate onto the lipid membrane in a similar fashion as evidenced in the case of DPPC monolayers.

Feasibility for development of membrane-based bioanalytical devices for metal determination

In this study, we also investigated whether the binding interaction between the chimeric Cd-binding GFP and lipid monolayers could potentially be used for the development of membrane-based bioanalytical devices for metal determination. These approaches include the effects of metal ions, particularly cadmium ions, on the fluorescence emission of immobilized chimeric Cd-binding GFP onto the DPPC monolayer and codetermination of metal ions with specific ligands. For the former, the His6CdBP4GFP was incorporated onto the DPPC monolayer, and the pressure was then increased to 20 mN/m in order to enhance the fluorescence emission due to reduction of liquid area prior to the addition of cadmium ions into the subphase. In our previous findings, we reported that metal ions exerted their suppressing effect on the fluorescence emission of purified chimeric GFPs (Prachayasittikul et al. 2000). However, in this study using lipid-bound protein, no effect on the epifluorescence pattern was observed following the

Table 1 Codetermination of Zn^{2+} and Cu^{2+} by chimeric GFPs and immobilized-metal-affinity chromatography

Metal ions	Chimeric proteins	Linear corresponding range (μmol)
Zn^{2+}	CdBP4GFP	2 to >5
Zn^{2+}	His6GFP	1 to >5
Cu^{2+}	CdBP4GFP	0.1 to >0.5
Cu^{2+}	His6GFP	0.05 to >0.5

addition of cadmium ions. Two possible explanations may be considered: (1) formation of complexes between the cadmium ions and the remaining protein in the subphase, as evidenced by the precipitation of chimeric protein beneath the lipid monolayer and (2) the disturbance of the membrane monolayer by the cadmium ions (Deleers et al. 1986; Sorensen et al. 1985).

Beyond these limitations, the difficulty of replacing a clear new buffer solution has to be taken into account if biosensor applications are to be developed. To overcome this problem, incorporation of the chimeric Cd-binding GFPs onto the lipid monolayers needs to be transferred to the solid supports via Langmuir-Blodgett transfer (Bourdos et al. 2000). These solid supported membranes can then be applied further as a biochip for direct quantification of metal ions via the immobilized Cd-binding GFPs on an optical sensor. For the latter, we have extrapolated a useful application of metal-chelating lipid as a specific ligand for codetermination of different metal ions. Based on our previous findings, estimation of a single metal in a system could be performed by immobilization of the metal onto a metal-binding matrix (Prachayasittikul et al., unpublished data). Therein, we used the IMAC gel as a ligand for codetermination of zinc and copper ions. Various concentrations of either zinc or copper ions were immobilized onto the IMAC column. Available metal ions could then be recognized using purified chimeric CdBP4GFP or His6GFP. Linear correlation between metal concentration and fluorescent intensity activity was detected.

Table 1 summarizes the quantity of Zn^{2+} and Cu^{2+} that could be analysed by such a system. The two chimeric GFPs denoted a similar range for metal quantification via IMAC. The amounts of Zn^{2+}, ranging from 1–2 up to 5 μmol, or Cu^{2+}, ranging from 0.05–0.1 up to 5 μmol, that were retained on the column could be detected. This also corresponded with the concentration of metal loaded onto the IMAC gel. Owing to this low sensitivity, it is necessary to take into account the capacity and susceptibility for binding metal ions to the IMAC-gel. Searching for a new ligand to enable the development of metal binding had to be geared for future tasks. Our findings indicate that the metal-chelating lipids show high potential for the application of membrane-based sensors for codetermination of metal ions via an optical sensor (Klee et al. 1995; Kostov et al. 2000) or quartz crystal microbalance (Pignataro et al. 2000; Wegener et al. 1999) in the future.

Acknowledgements This work was supported by the Deutsche Forschungsgemeinschaft (DFG) and the Bundesministerium für wirtschaftliche Zusammenarbeit und Entwicklung (Federal Ministry for Economic Cooperation and Development; BMZ) (grant no.GA233/19–1,2). This project was also supported by a grant from the annual budget of Mahidol University for collaborative research between Germany and Thailand.

References

Bakker E, Telting-Diaz M (2002) Electrochemical sensors. Anal Chem 74:2781–2800

Bevan DR, Worrel WJ, Barfield KD (1983) The interaction of Ca^{2+}, Mg^{2+}, Zn^{2+}, Cd^{2+}, and Hg^{2+} with phospholipid bilayer vesicles. Colloids Surfaces 6:365–376

Bontidean I, Berggren C, Johansson G, Csoregi E, Mattiasson B, Lloyd JR, Jakeman KJ, Brown NL (1998) Detection of heavy metal ions at femtomolar levels using protein-based biosensors. Anal Chem 70:4162–4169

Bourdos N, Kollmer F, Benninghoven A, Ross M, Sieber M, Galla HJ (2000) Analysis of lung-surfactant model systems with time-of-flight secondary ion mass spectrometry. Biophys J 79:357–369

Burdette SC, Walkup GK, Spingler B, Tsien RY, Lippard SJ (2001) Fluorescent sensors for Zn^{2+} based on a fluorescein platform: synthesis, properties and intracellular distribution. J Am Chem Soc 123:7831–7841

Celia H, Wilson-Kubalek E, Milligan RA, Teyton L (1999) Structure and function of a membrane-bound murine MHC class I molecule. Proc Natl Acad Sci USA 96:5634–5639

Choi JW, Nam YS, Park SJ, Lee WH, Kim D, Fujihira M (2001) Rectified photocurrent of molecular photodiode consisting of cytochrome c/GFP hetero thin films. Biosensors Bioelectronics 16:819–825

Cooper MA (2002) Optical biosensors in drug discovery. Nat Rev Drug Discov 1:515–528

Cyr DM, Langer T, Douglas MG (1994) DnaJ-like proteins: molecular chaperones and specific regulators of Hsp70. Trends Biochem Sci 19:176–181

Da Silva E, Foley M, Dluzewski AR, Murray LJ, Anders RF, Tilley L (1994) The *Plasmodium falciparum* protein RESA interacts with the erythrocyte cytoskeleton and modifies erythrocyte thermal stability. Mol Biochem Parasitol 66:59–69

Deleers M, Servais JP, Wulfert E (1986) Neurotoxic cations induce membrane rigidification and membrane fusion at micromolar concentrations. Biochim Biophys Acta 855:271–276

Dietrich C, Schmitt L, Tampe R (1995) Molecular organization of histidine-tagged biomolecules at self-assembled lipid interfaces using a novel class of chelator lipids. Proc Natl Acad Sci USA 92:9014–9018

Dorn IT, Pawlitschko K, Pettinger SC, Tampe R (1998) Orientation and two-dimensional organization of proteins at chelator lipid interfaces. Biol Chem 379:1151–1159

Dufourcq J, Faucon JF (1977) Intrinsic fluorescence study of lipid-protein interactions in membrane models. Binding of melittin, an amphipathic peptide, to phospholipid vesicles. Biochim Biophys Acta 467:1–11

Falchuk KH, Hilt KL, Vallee BL (1988) Determination of zinc in biological samples by atomic absorption spectrometry. Methods Enzymol 158:422–434

Gardner MJ, Tettelin H, Carucci DJ, Cummings LM, Aravind L, Koonin EV, Shallom S, Mason T, Yu K, Fujii C, Pederson J, Shen K, Jing J, Aston C, Lai Z, Schwartz DC, Pertea M, Salzberg S, Zhou L, Sutton GG, Clayton R, White O, Smith HO, Fraser CM, Hoffman SL, et al. (1998) Chromosome 2 sequence of the human malaria parasite *Plasmodium falciparum*. Science 282:1126–1132

Girault L, Boudou A, Dufourc EJ (1998) ^{113}Cd-, ^{31}P-NMR and fluorescence polarization studies of cadmium(II) interactions with phospholipids in model membranes. Biochim Biophys Acta 1414:140–154

Grandbois M, Dufourcq J, Salesse C (1996) Study of the synergistic action of phospholipase A2 and melittin in the hydrolysis of phospholipid monolayers. Thin Solid Films 284–285:743–747

Isarankura Na Ayudhya C (2000) Engineering of chimeric protein for binding to metal ions. PhD Thesis, Mahidol University, Bangkok, Thailand

Javanbakht M, Shabani-Kia A, Darvich MR, Ganjali MR, Shansipur M (2000) Cadmium(II)-selective membrane electrode based on a synthesized tetrol compound. Anal Chim Acta 408:75–81

Kahle C, Koch PJ, Durr W, Kastowsky M, Bradaczek H (1996) Active penetration of charged peptides into monomolecular films of deep rough mutant lipopolysaccharide. Thin Solid Films 284–285:802–804

Keusgen M (2002) Biosensors: new approaches in drug discovery. Naturwissenschaften 89:433–444

Klee B, John E, Jahnig F (1992) A biosensor based on the membrane protein lactose permease. Sensors Actuators B 6:376–379

Klee B, Duveneck GL, Oroszlan P, Ehrat M, Widmer HM (1995) A model system for the development of an optical biosensor based on lipid membranes and membrane-bound receptors. Sensors Actuators B 29:307–311

Knauer K, Behra R, Sigg L (1997) Adsorption and uptake of copper by the green alga *Scenedesmus subspicatus* (chlorophyta). J Phycol 33:596–601

Kostov Y, Albano CR, Rao G (2000) All solid-state GFP sensor. Biotechnol Bioeng 70:473–477

Kubalek EMW, Brown RE, Celia H, Milligan RA (1998) Lipid nanotubes as substrates for helical crystallization of macromolecules. Proc Natl Acad Sci USA 95:8040–8045

Lehmann M, Riedel K, Adler K, Kunze G (2000) Amperometric measurement of copper ions with a deputy substrate using a novel *Saccharomyces cerevisiae* sensor. Biosensors Bioelectronics 15:211–219

Lis LJ, Lis WT, Parsegian VA, Rand RP (1981) Adsorption of divalent cations to a variety of phosphatidylcholine bilayers. Biochemistry 20:1771–1777

Lu YJ, He Y, Sui SF (2002) Inositol hexakisphosphate (InsP6) can weaken the Ca(2+)-dependent membrane binding of C2AB domain of synaptotagmin I. FEBS Lett 527:22–26

MacRitchie F (1986) Spread monolayers of proteins. Adv Colloid Interface Sci 25:341–385

Maman N, Dhami S, Phillips D, Brault D (1999) Kinetic and equilibrium studies of incorporation of di-sulfonated aluminum phthalocyanine into unilamellar vesicles. Biochim Biophys Acta 1420:168–178

Matsuzaki K, Sugishita K, Harada M, Fujii N, Miyajima K (1997) Interactions of an antimicrobial peptide, magainin 2, with outer and inner membranes of Gram-negative bacteria. Biochim Biophys Acta 1327:119–130.

Mejare M, Ljung S, Bulow L (1998) Selection of cadmium-specific hexapeptides and their expression as OmpA fusion proteins in *Escherichia coli*. Protein Eng 11:489–494

Norde W (1986) Adsorption of proteins from solution at the solid–liquid interface. Adv Colloid Interface Sci 25:267–340

Pignataro B, Steinem C, Galla HJ, Fuchs H, Janshoff A (2000) Specific adhesion of vesicles monitored by scanning force microscopy and quartz crystal microbalance. Biophys J 78:487–498

Prachayasittikul V, Isarankura Na Ayudhya C, Mejare M, Bulow L (2000) Construction of a chimeric histidine6-green fluorescent protein: role of metal on fluorescent characteristic. Thammasat Int J Sc Tech 5:61–68

Prachayasittikul V, Isarankura Na Ayudhya C, Bulow L (2001) Lighting *E. coli* cells as biological sensors for Cd^{2+}. Biotechnol Lett 23:1285–1291

Rishpon J (2002) Electrochemical biosensors for environmental monitoring. Rev Environ Health 17:219–247

Rogers KR, Valdes JJ, Eldefrawi ME (1989) Acetylcholine receptor fiber-optic evanescent fluorosensor. Anal Biochem 182:353-359

Savory J, Herman MM (1999) Advances in instrumental methods for the measurement and speciation of trace metals. Ann Clin Lab Sci 29:118–126

Schmidt CF, Zimmermann RM, Gaub HE (1990) Multilayer adsorption of lysozyme on a hydrophobic substrate. Biophys J 57:577–588

Shank-Retzlaff ML, Raner GM, Coon MJ, Sligar SG (1998) Membrane topology of cytochrome P450 2B4 in Langmuir-Blodgett monolayers. Arch Biochem Biophys 359:82–88

Sorensen EM, Acosta D, Nealon DG (1985) Effects of cadmium and calcium on the fluidity of plasma membranes. Toxicol Lett 25:319–326

Tacnet F, Ripoche P, Roux M, Neumann JM (1991) ^{31}P-NMR study of pig intestinal brush-border membrane structure: effect of zinc and cadmium ions. Eur Biophys J 19:317–322

Tauriainen S, Karp M, Chang W, Virta M (1998) Luminescent bacterial sensor for cadmium and lead. Biosens Bioelectron 13:931–938

Thompson JD, Higgins DG, Gibson TJ (1994) CLUSTAL W: improving the sensitivity of progressive multiple-sequence alignment through sequence weighting, position-specific gap penalties and weight matrix choice. Nucleic Acids Res 22:4673–4680

Vercoutere W, Akeson M (2002) Biosensors for DNA sequence detection. Curr Opin Chem Biol 6:816–822

Wegener J, Janshoff A, Galla HJ (1999) Cell adhesion monitoring using a quartz crystal microbalance: comparative analysis of different mammalian cell lines. Eur Biophys J 28:26–37